PREVENTION AND INVESTIGATIONS OF CORE DEGRADATION IN CASE OF BEYOND DESIGN ACCIDENTS OF THE 2400 MWTH GAS-COOLED FAST REACTOR

F. Bertrand¹, V. Gatin¹, F. Bentivoglio², C. Gueneau³

¹ CEA, DEN, DER, SESI, Cadarache, F-13108 Saint Paul Lez Durance, France

² CEA, DEN, DER, SSTH, Grenoble, F-38054 Grenoble, France

³ CEA, DEN, DPC, SCP, Saclay, F-91191 Gif Sur Yvette, France

frederic.bertrand@cea.fr

Abstract

The present paper deals with studies carried out to assess the ability of the core of the Gas Fast Reactor (GFR) to withstand beyond design accidents. The work presented here is aimed at simulating the behaviour of this core by using analytical models whose input parameters are calculated with the CATHARE2 code. Among possible severe accident initiators, the Unprotected Loss Of Coolant Accident (ULOCA of 3 Inches diameter) is investigated in detail in the paper with CATHARE2. Additionally, a simplified pessimistic assessment of the effect of a postulated power excursion that could result from the failure of prevention provisions is presented.

1. Introduction

After a brief presentation of the Gas cooled Fast Reactor (GFR) as pre-designed by CEA in 2009 [1], taken as the reference in the studies presented here, the first part of the paper deals with the possibility of prevention of core degradation in case of a bounding small break ULOCA (SB-ULOCA). Considering the overheating conditions experienced by the fuel, the growth of the interaction zone (within the fuel/liner/cladding system) has been assessed by means of a material interaction model. In the second part of the paper, the consequences of a neutronic reactivity uncontrolled insertion are calculated thanks to simplified analytical tools developed for this purpose and taking into account the coupling between thermalhydraulics, thermochemistry and neutronics. Finally, the results of the aforementioned studies are drawn in the whole picture of the GFR preliminary safety analysis in order to assess the capability of prevention and of mitigation of severe accidents of the GFR concept as a complement of previous papers [1], [2] and [3].

2. The CEA 2400 MWth Gas-Cooled Fast Reactor

The GFR represents a promising and attractive fourth generation (GEN IV) concept, combining the benefits of a fast spectrum and of a high temperature (~ 850°C). The GFR concept is clearly innovative compared to other reactor concepts and no demonstrator has ever been built. The project of an industrial GFR has to address key R&D challenges, especially regarding, the fuel technology and core performance and the safety (in particular the Decay Heat Removal (DHR) issue).

2.1. Main features of the reactor

This paper is dedicated to severe accidents approach and related studies. The detailed GFR design is presented in reference [1], and only the features useful to the understanding of the accident studies are presented here.

2.1.1. Main design options

The operating point of the 3-loops reactor at full nominal power enables to convert the 2400 MWth delivered by the core in 1100 MWe, partly by secondary circuit turbomachineries (TM) (auxiliary alternators: 3 x 130 MWe) and partly by a steam turbine (main alternator: 1 x 730 MWe) settled in the ternary circuit (Fig 1). The resulting cycle efficiency is very close to 45 %. The secondary circuit is filled with a mixture of helium (to favour the heat exchanges) and nitrogen (to favour the efficiency and the design of the turbomachineries); the ternary circuit is filled with water, vaporized in 3 steam generators according to a classical Rankine cycle. The primary system arrangement [1] includes the reactor vessel, the 3 main primary loops delivering a total flow rate of 1020 kg/s in the downcomer (PCS loops) and their heat exchangers (IHX) as well as the DHR loops permitting to cool the core in accidental situations. Actually, there are three loops, so-called, Reactor High Pressure cooling system (RHP) and two loops for the low pressure situations (RLP) not used in the transient calculated in this paper.

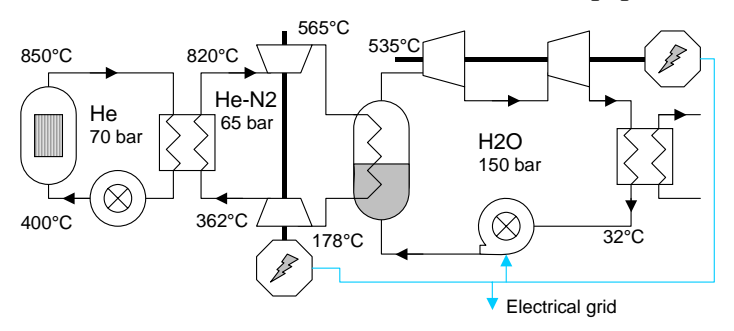
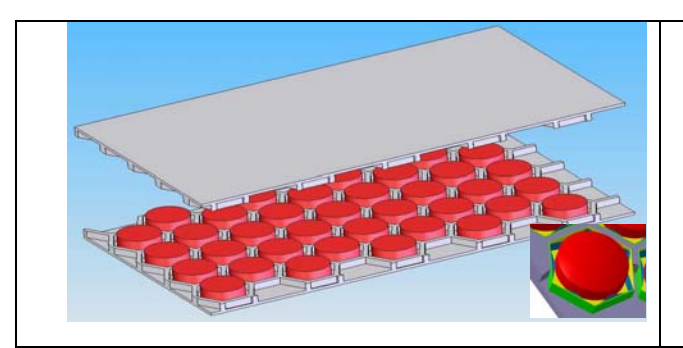
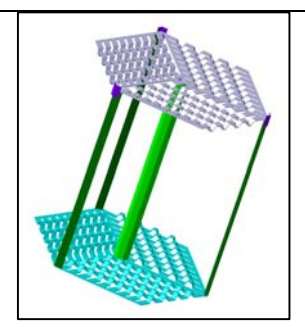


Fig. 1 Nominal operating point of the GFR

Moreover, all the previous components are enclosed in a close containment (CC) which keeps the primary inventory in case of LOCA. The CC is filled with nitrogen at 1 bar. Two fuel concepts are currently under investigation: a plate type and a more classical pin type. The present paper only deals with the plate type developed earlier than the other one (Fig 2). The plate-type fuel element is an innovative concept based on two ceramic plates which encloses a honeycomb structure containing the fuel cylindrical pellets. The plate consists in uraniumplutonium-minor actinide carbide, (U,Pu,MAs)C for pellets, composite SiC-SiCf for thin plates (clad) and SiC for the honeycomb structure. It appeared necessary to add a leak-tight barrier to prevent the Fission Products (FP) diffusion through the clad. The current reference choice for this internal liner is a 50 µm layer of W-14Re. At the hot spot of the core, the clad temperature is equal to 1030°C and the fuel temperature is about 1290°C in nominal conditions. The plates are arranged in baskets superposed in hexagonal tubes (TH) permitting to differentiate the flow rate depending on the power factor distribution within the core. The height of the core is of 2.35 m and its diameter is of 3.8 m, thus corresponding to a power density of about 90 MW/m³. The head loss across the core has been minimized at a value of 1.4 bars at the nominal regime in order to favour natural circulation in DHR regime.





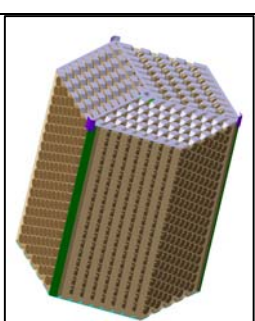


Fig. 2 Fuel assembly sketch

Table 1 Core main neutron features

	First cycle	Equilibrium
TRU enrichment (%)	17.3	18.2
Doppler Constant* ** (pcm)	-1331 / -905	-1283 / -837
He depressurization* (pcm)	259 / 282	309 / 307
Delayed neutron fraction* (pcm)	389 / 349	355 / 342

^{*} BOL / EOL, ** at nominal temperature

2.1.2. Main options and features dealing with the safety of the GFR

The reactivity control is firstly insured by a favourable natural behaviour of the core resulting from the neutron reaction feedback (Tab 1). In particular, the coolant being largely transparent to neutrons: the voiding effect is lower than 1\$ without a threshold effect due to a phase change like with liquid coolants. Furthermore, the Doppler coefficient is large for a fast reactor, resulting in a stabilizing effect. The reactor shutdown can be actuated by means of control rod drive mechanisms located at the bottom of the vessel, in the coldest environment. The absorber rods are located above the core. Thanks to this design, the practical elimination of a control rod ejection accident is targeted. The tightness of the first barrier and the keeping of core coolable geometry rely mainly on the fuel element based on refractory materials with high thermal conductivity and high temperature melting point, with the ability to ensure FP confinement up to a fairly high temperature. Considering the power density of the GFR core and its low thermal inertia (compared to the HTR) and that of the coolant as well (compared to the SFR), the decay heat removal relies on a gas circulation (natural circulation as far as possible) across the core but not on solutions based on thermal inertia plus conduction/radiation. The DHR operating depends on the accidental situation to face (Figure 3 and Figure 4). The selected combination of systems takes into account the two main accidental situation families: the pressurized situations (intact primary boundary) and the depressurization situations resulting from a LOCA. The means represented in the upper part of the sketch are used in priority if available, depending on the pressure range considered and on the means represented below being used if those above have failed. In addition, the situation related to a primary pressure reaching around 0.1 Mpa, corresponding to a combination of LOCA and a leak of the CC, has been considered. Such architecture of the DHR system has been proved to cope with the safety objective of the GFR with a level 1 PSA [4].

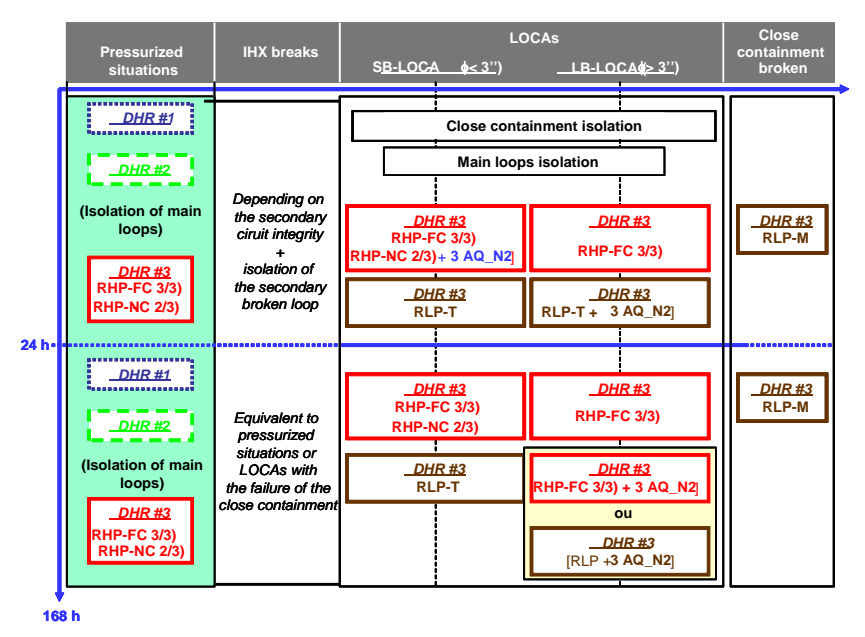


Fig. 3 Sketch of the DHR operation (DHR#1 in blue on Fig.4, DHR#2 in green on fig.4, DHR#3 (dedicated means in CC) on Fig.4)

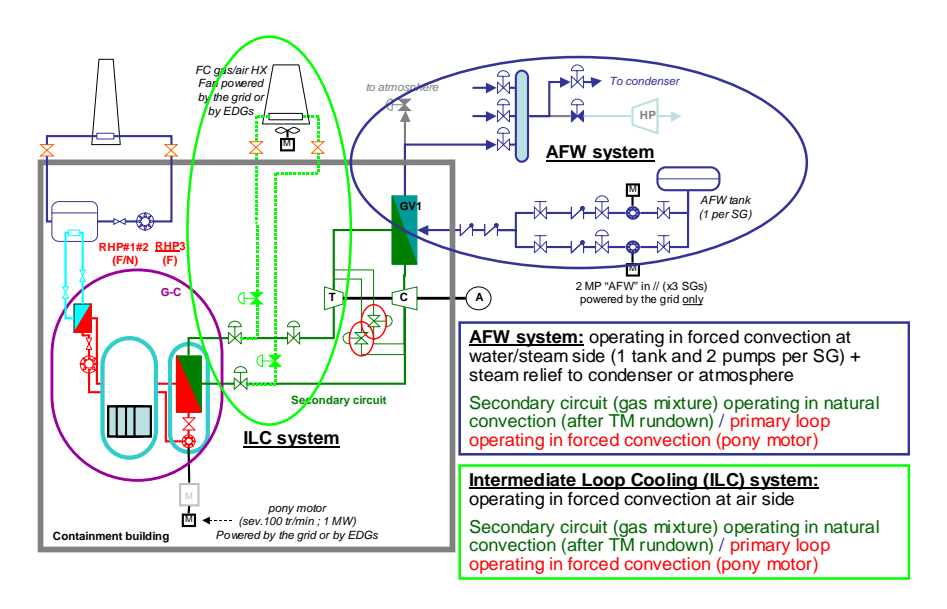


Fig. 4 Sketch of various DHR means

It is worth noticing that the DHR based on natural circulation with a heavy gas for small breaks relies on the presence of the CC insuring a back-up pressure of about 1 MPa. This CC permits also to dimension DHR blowers with a low power, compatible with an emergency electrical power supply, delivered by Diesel engines.

3. Prevention of core degradation in case of a small break unprotected loss of coolant (SB-ULOCA)

Among the possible severe accident initiators identified previously [3] for the GFR, the capability of control a SB-ULOCA without loosing the coolability of the core is still to investigate and this section deals with this issue by focusing on the bounding 3 inches break. Actually, this break size has been determined as the upper limit of the break diameter allowing the decay heat removal in natural convection thanks to nitrogen injection (see [2] and [3]) for within the design basis domain. It also consists in the limit beyond which core flow rate reversal occurs and induces a fast over-cooling of the upper part of the core for large breaks. For these reasons it has been retained as the bounding third category SB-LOCA, the larger breaks requiring another control strategy and safety criteria.

3.1 Thermalhydraulic transient calculated with the CATHARE2 code

The calculations presented in this part have been carried out with the CATHARE2 code v25 2 ([5], [6]) and the modelling of the GFR with the code is presented in [7]. The DHR strategy as indicated on Figure 4 is foreseen to cool the core after the reactor scram. This latter actuates the DHR sequence with a core cooling with the normal loops whose primary flow rate is delivered by a pony motor and secondary flow rate by natural convection (DHR#1 and DHR#2) or by the dedicated loops (DHR#3) depending on the primary pressure and on the availability of the power supply. In the transient calculated here, since the reactor shutdown failed the heat removal procedure relies on the normal loops operating with their blowers and turbomachineries operating close to their nominal rotation speed (DHR#1). However, due to the increase of the core power at the beginning of the transient (helium density effect), the power delivered by the turbomachinery to the alternator becomes too high and this latter is disconnected. As a consequence, the turbomachinery speed of the secondary loops is regulated thanks to their bypass valve and an unacceptable overheating of the IHX and of the upper plenum materials is reached in several minutes. As already shown in [3], a heavy gas injection enhances the core cooling in a natural convection flow but in a forced convection regime as well. The injection is performed by 3 accumulators of 540 m³ filled with nitrogen at 75 bars and is triggered when the primary pressure reaches 14 bars in case of protected transient associated to the loss of all active cooling systems [3]. Nevertheless, the gas changing in the core has to be taken into account in a neutron point of view as well as its density changing. Therefore, the transient calculated in this section takes into account a core cooling by the power conversion system (PCS loops) associated to nitrogen injection at a primary pressure that was optimized thanks to the calculations. It is to note that the influence of the presence of a mixture of nitrogen and helium in the circuits is taken into account in the performance maps of the rotating machines.

3.1.1 Modelling and influence of the neutron effect of nitrogen injection

The feed-back reactivity effects due to the Doppler effect and due to the density variation of helium were taken into account in the reference CATHARE2 input deck of the GFR [7]. Additionally, the less important moderating effect of nitrogen compared to helium should also been taken into account. Two effects are indeed of importance and have been calculated by using the ERANOS neutron code [8]. The first is the volumic fraction of nitrogen and helium in the

core that changes very fast as soon as the accumulator relief is triggered because He is replaced by N_2 thanks to the leak through the primary break (Figure 6). The second effect is the density changing of the gas mixture (Figure 5) due to N_2 injection that takes place one order of magnitude more slowly than volumic fraction changing. Therefore, it has been assumed that the neutron impact of the evolution of the gas composition could be modelled in CATHARE2 thanks to an external reactivity insertion deduced from ERANOS calculation results and fitting the gas composition calculated with CATHARE2: namely 0,115 \$ during the 6 first seconds after the accumulator opening and 4.5 cents during the following 80 seconds. Moreover, by considering that the voiding effect acts later on than the gas composition changing it is taken into account at the beginning of the injection by dividing the voiding coefficient by the ratio of the slopes of the blue curve to the orange curve of Figure 5. This assumption penalizes the calculation because it reduces the neutron benefit of gas density increase earlier than if the voiding coefficient had match exactly the mixture composition in the first seconds of the injection transient.

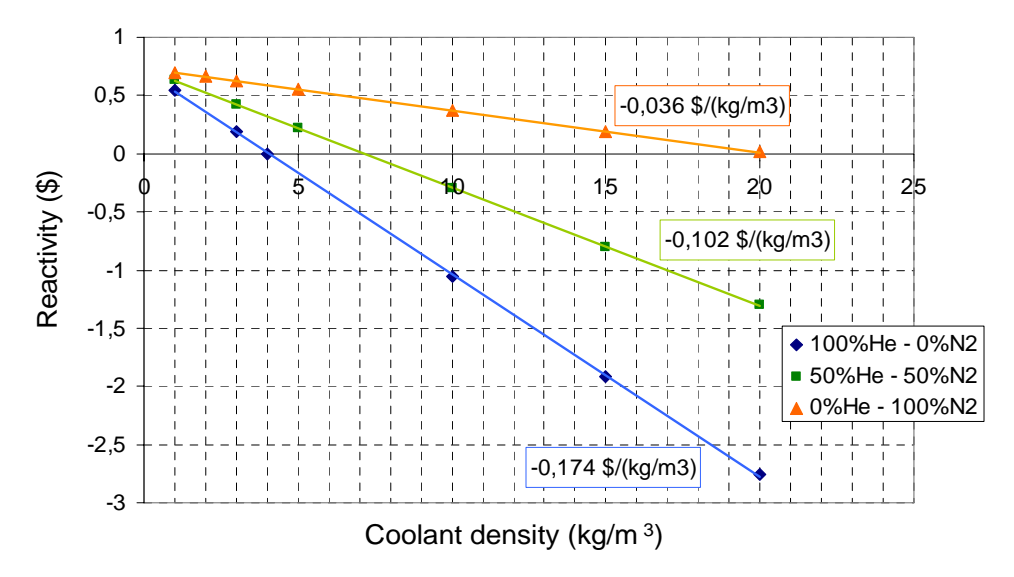


Fig. 5 Reactivity variation as a function of the composition of the gas mixture and its density calculated with the ERANOS code

Assuming the triggering of the accumulator at 14 bars and a transient initiating by a 3 inches break combined with the failure of the reactor scram, the neutron effect of the N_2 injection leads to a equilibrium core power close to the nominal power whereas it leads to core power lower than 100 MW by only considering helium in the core (Figure 6). The major effect is the changing of the voiding coefficient (voiding effect) compared to the volume fraction of gases in the core (Figure 7). As shown by this calculation results, the opening pressure of the accumulator has to be increased in order to lower the maximum temperature reached by the cladding. Therefore, the sensitivity of the maximum cladding temperature and of the core power to the pressure of the accumulator relief has been investigated. As a result, the optimal relief pressure has been calculated around 40 bars in order to avoid a temperature escalation above 1850° C, that is the liquefaction temperature of the system cladding/liner of the fuel assembly. This later has been assessed by means of thermodynamic equilibrium calculations carried out with the Thermocalc code [9] whose data base (FUELBASE) validation is under way with

analytical tests carried out at CEA [10]. The power peak induced by the N_2 injection increases when the relief pressure increases but without any significant effect on the overheating of the core materials. The equilibrium power is the same whatever the injection pressure is. The overheating depends in the short term on the injection pressure (period before injection) and on the back-up pressure on the long term of the transient (after N_2 injection) that is the same if the accumulator inventory remains the same.

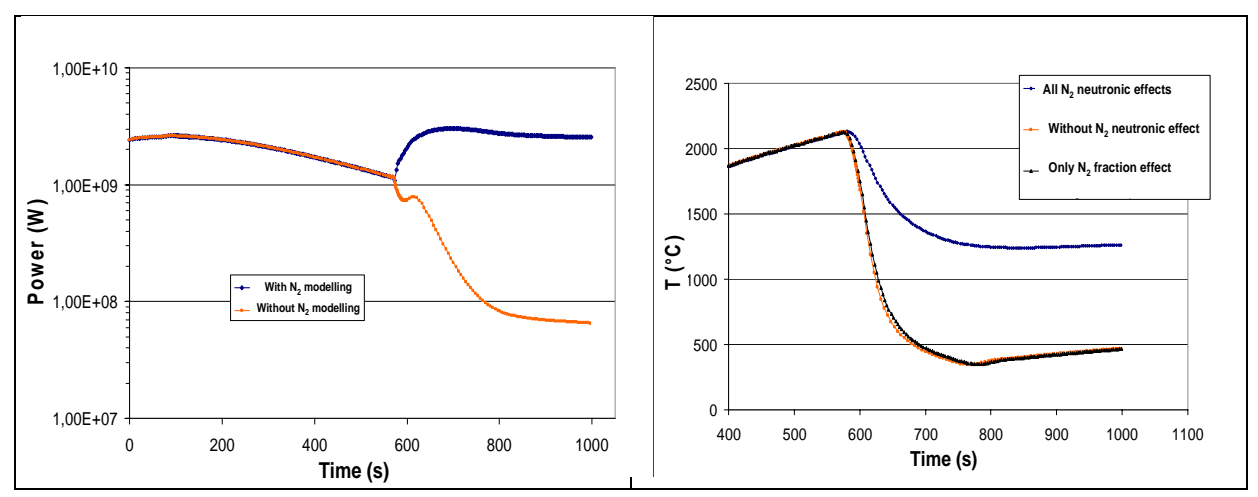


Fig. 6 Impact of the modelling of the N_2 neutron effect on the core power and on the cladding temperature evolution

3.1.2 Possibility to control the accident in order to minimize the core material overheating

Considering the keeping of the operating parameters of the reactor within a realistic range (flow rates in the primary circuit, turbomachinery speed, flow rate of steam generator (SG) feed water and title of the steam), the minimization of the core overheating has been studied in order to fulfil the following criteria enabling the geometry of the core to be kept coolable: a long term cladding temperature remaining below 1850°C (eutectic cladding/liner) and a short term cladding temperature remaining below 2000°C. The enhancement of the core cooling is obtained by: increasing the rotation speed of the main blowers of 20% once the break occurs, opening 4 accumulators (instead of 3 in the reference case) and increasing the power removed by the SG. This increase has been simulating by increasing the SG feed water and by reducing the SG outlet pressure from 150 to 100 bars. As soon as the power transferred by the TM to the alternators exceeds 14% of its nominal value, it is disconnected and the TM keeps its nominal speed thanks to a regulated opening of their by-pass lines (Figures 4 and 7). As a result, the overheating of the fuel and of the cladding are respectively limited to 2000°C and 1800°C in the hottest zone of the core (Figure 7). Moreover, during the first hour, the 4th category criteria are not exceeded (upper plenum temperature < 1250°C and cladding temperature < 1600°C). However, this accident management with the relief of 4 accumulators would imply a reinforced dimensioning of the CC or its external cooling because its pressure reaches 15 bars during a short period of the transient. As a conclusion, such a transient could be controlled in order to provide a comfortable grace delay in order to actuate the reactor shutdown. Another way to limit the thermomechanical loading of the core and of the structures would be to lower the core power by injecting a neutron absorber within the core. Such a calculation has been carried out by considering a low fraction of He³ in the accumulator and no matter the prohibitive cost of this compound the cladding temperature can be maintained below the 4th category criteria with any particular cooling enhancement adopted in the calculation presented on Figure 7 because the core power would be twice time lower with only 5 % of this absorbent in the accumulator. However, the results presented before should be considered only as preliminary results that would be to confirm with a more refined modelling of the secondary and ternary loops of the GFR, especially regarding the TM modelling in CATHARE2 (more consolidated performance maps) and with a more refined modelling of the core reactivity feedback.

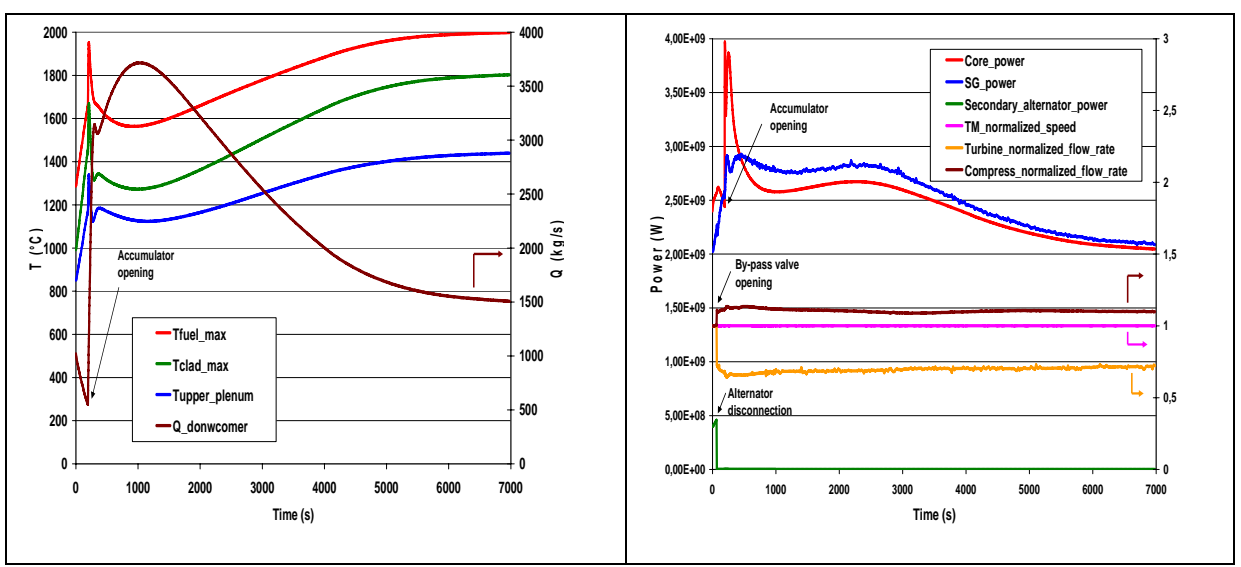


Fig. 7 Transient behaviour of the GFR in case of 3 inches unprotected SB-LOCA (enhancement of cooling by increasing the speed of the primary blowers and SG operating)

3.2 Assessment of the physico-chemical interactions within the fuel/liner system

The calculation of the material interactions is performed in this part for the 3 inches SB-LOCA calculated with the system assumptions retained in the previous section. The thermal evolution of the claddings located in the higher part of the core calculated with CATHARE2 code are used as an input parameter of the interaction models that provide the thickness of liner consumed on the fuel side as well as on the cladding side. As a result, these calculations enable the grace delay available to keep the core geometry to be calculated.

3.2.1 Modelling of the growth of the fuel/liner interaction zone

The reference material retained for the liner consists in a W-5%Re layer whose thickness is equal to 50 μ m (Figure 8). Eremeev [11] proposed a simple parabolic law in order to estimate the growth of the interaction zone as a function of time and of the temperature (diffusion limited phenomenon). The limitation of this model deals with its validation on tests performed on UC/W systems that did not include the influence of Pu included in the GFR fuel. Thermodynamic equilibrium calculations indicate that a eutectic appears in the fuel/liner system around 1880°C. Beyond this temperature, the Eremeev model is no more valid because it deals with solid/solid systems. According to the model, the thickness of the reaction zone made of W_2C can be expressed as:

$$e = 2a\sqrt{D t}$$
 (1)

with
$$D(T) = 18.3 \exp(-\frac{392840}{RT})$$
 (2)

where a is a factor depending on the initial carbon concentration in the fuel, D ($\rm m^2/s$) is the diffusion coefficient of C in the W₂C layer, R is the perfect gas constant and T is the temperature. The parameters a and D depending on the temperature, they have been calibrated on thermodynamic calculations for temperature ranging from 1200°C to 1850°C by steps of 50°C. By using equations (1) and (2) between two time steps of the CATHARE2 calculation results presented in section 3.1.2, the integrated thickness of the reaction zone can be calculated in various regions of the core. As soon as the temperature exceeds 1880°C, the Eremeev model being no more applicable, the growth is stopped and the reaction zone is supposed to be liquid (eutectic point of the fuel/liner system).

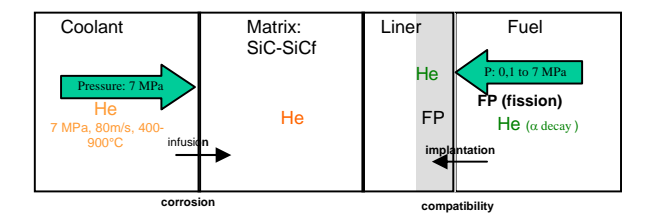


Fig. 8 Sketch of the arrangement of the fuel/liner/cladding system

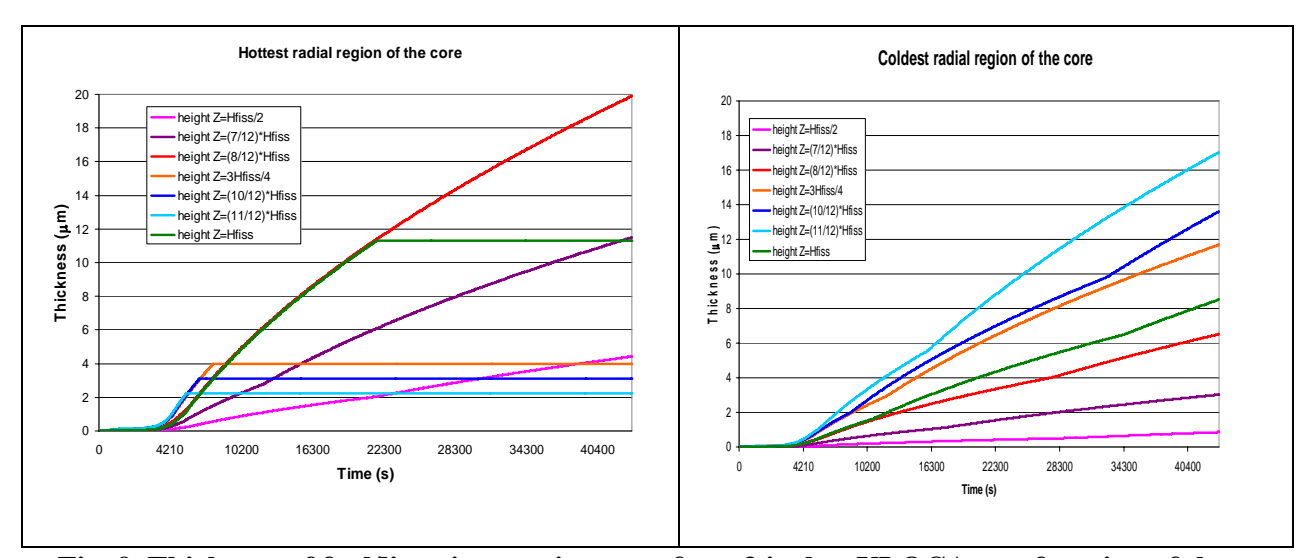


Fig. 9 Thickness of fuel/liner interaction zone for a 3 inches ULOCA as a function of the axial location in the core

Figure 9 shows that in the hottest radial region of the core (central channels in the CATHARE2 modelling), the liner liquefaction at its interface with the fuel is reached after approximately 1.5 h at the hot spot whereas approximately 1/3 of the liner thickness is consumed by the

interaction without any liquefaction in the outer radial region of the core (Figure 9, right side). The consumption of the liner on its outer interface with the cladding should be also assessed.

3.2.2 Modelling of the growth of the liner/cladding interaction zone

Experimental tests presented in [12] have shown that the growth of the reaction zone from an initial thickness equal to x_0 to x during a duration t follows a parabolic law can be expressed:

$$(x - x_0)^2 = K_n t$$
 (3)

with

$$K_p = K_0 \exp(-\frac{505780}{RT})$$
 (4)

and where $K_0 = 1.1 \ 10^5 \ cm^2/s$. The results of the reaction zone growth calculations based on the same temperature evolution as in sub-section 3.2.1, indicates that in 7500 s the totality of the liner has been consumed at the hot spot of the core only by the liner/cladding interaction occurring in solid phase. Beyond the degradation of its mechanical properties due to the growth of the interaction zone, it would be interesting to assess its ability to remain tight and to keep the initial core geometry despite the absence of liquefaction before the total consumption of the liner. Finally, by considering the degradation of the liner from both sides, it has been fully consumed after 2 hours when it is not liquefied before in its inner face.

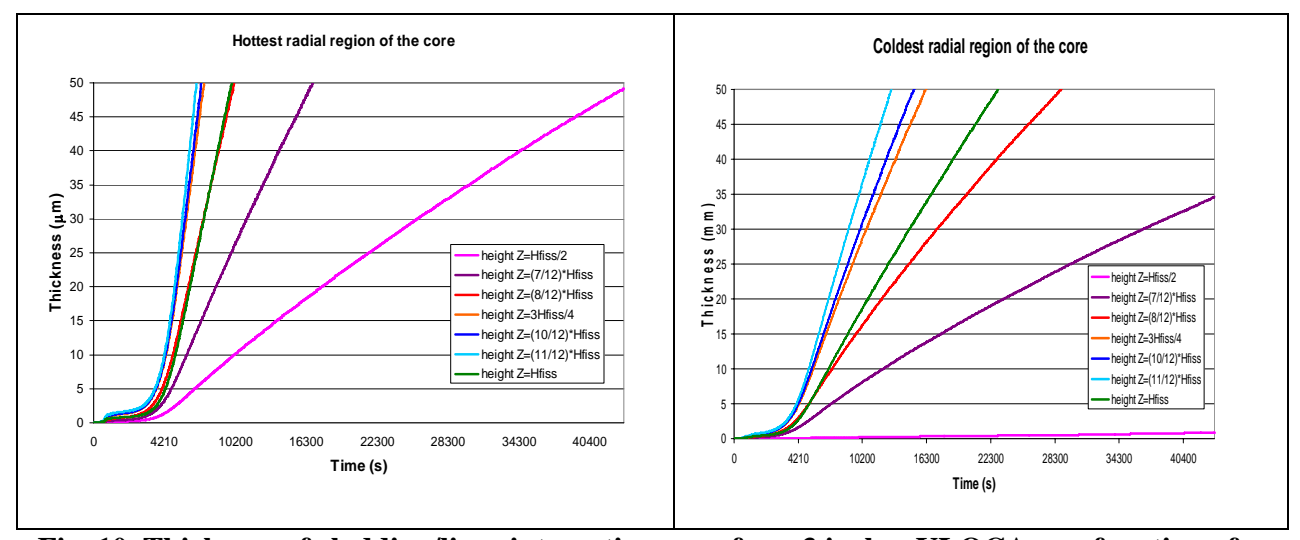


Fig. 10 Thickness of cladding/liner interaction zone for a 3 inches ULOCA as a function of the axial location in the core

As a conclusion, the strategy proposed to control the bounding SB-LOCA combined with the reactor shutdown failure enables to shutdown the reactor within a time period ranging from 1.5 to 2 hours after the accident without any loss of a coolable geometry of the core. The possible evolution of the accident after this delay or before this delay in case of failure of the cooling strategy proposed in sub-section 3.1.2 is assessed in the next part of the paper.

4. Simplified analytical assessment of vessel pressurization in case of power excursion

Considering various scenarios leading to material relocation, one can have an overall core axial compaction leading to a decrease of the neutron leaks that would induce a reactivity increase. Reference [3] provides examples of reactivity insertion in case of axial compaction of a part of the core. More precisely, in case of segregation between the cladding materials and the fissile materials, as soon as 7 assemblies are molten, the theoretical reactivity inserted based on ERANOS calculations would be about 7 \$ (1 \$ stands for delayed neutron fraction). Practically speaking, in accidents calculations performed for SFR concept [13] the net reactivity exceeds hardly 1 \$ because once the prompt criticality is reached, the materials are rapidly dispersed, thus stopping the power excursion. Among the various causes of power excursion that could occur (extension of a local cooling failure of the core, generalized overheating or absorber assemblies ejection, etc.), the paper is focused on fast power insertion leading to a large thermal energy release and therefore to core material boiling. The objective of those calculations deals with the pressurization of the vessel that would arise. The scenario considered later on could be obtained in case of an ULOCA calculated before without any mitigation action like delayed reactor scram for instance or with the failure of the strategy assessed in sub-section 3.1 to prevent a core degradation (in particular no N₂ injection). Then, the subsequent core degradation is supposed to be spatially coherent, thus leading to a large axial compaction of the core materials due to their relocation up to the power excursion.

4.1 Simplified modelling of the core power evolution

Assuming a very rough modelling of the power evolution thanks to a single group neutron assessment, the power evolution following a postulated reactivity insertion (Rho_{insert}) around 2 \$ has been considered. By various simplifications of the Nordheim equation [14] and by neglecting the neutrons emitted by disintegrations due to their long time constant compared to the prompt neutrons, the power evolution in case of high and sudden reactivity insertion can be approximated:

$$P(t) = P_0 \exp(\frac{Rho - \beta}{\ell}t)$$
 (5)

where P_0 is the core power before the reactivity insertion (assumed here to be the nominal power), Rho the reactivity, β the delayed neutrons fraction and \mathcal{I} the generation time of neutrons equal to 6. 10^{-7} s. Moreover, the only neutron feedback limiting the power excursion is conservatively assumed to be the Doppler effect because in case of fast and large reactivity increase, the fuel would melt before the cladding because the power is released in a quasi-adiabatic way into the fuel (no matter the physico-chemical interactions, considered to occur too slowly to have an impact) and would be dispersed only after cladding decomposition. As a result, the evolution of the reactivity during a time interval during which the mean temperature of the core increase from T up to T+dT can be expressed:

Rho = Rho_{insert} -
$$K_D \ln(\frac{T + dT}{T})$$
 (6)

with K_D the Doppler constant of the GFR core equal to 895 pcm.

4.2 Simplified modelling of the thermalhydraulic phenomena

The initial conditions of the primary circuit before the power excursion in case of ULOCA result from the depressurization of the primary circuit up to the equilibrium pressure insured by the CC that is equal to 5 bars in case of SB-LOCA. Therefore, assuming a constant intermediate temperature between the core materials and the vessel wall for the gas in the vessel (T_{gas}), any pressure evolution of the pressure P_{prim} in the primary circuit during a time step dt can be written:

$$P_{prim}(t+dt) = P_{prim}(t) + (dn_{vap} - (Q_{break}(t) / M_{av}(t)).dt). RT_{gas}/V_{prim}$$
(7)

with

$$Q_{break}(t) = C_d \cdot S_{break} \cdot P_{prim}(t) \cdot (M_{av}(t) \cdot \gamma/(R \cdot T_{gas}) \cdot f(\gamma)$$
(8)

for a sonic flow with $f(\gamma) = \left(\frac{2}{\gamma+1}\right)^{\frac{\gamma+1}{2(\gamma-1)}}$ and multiplied by a function non detailed here of the

pressure of the CC, of γ and of P_{prim} (t) in case of subsonic flow ([15] for instance). In equation (7), dn_{vap} stands for the mole number of core materials vaporized during the time step, M_{vap} for the average molar mass of the gaseous mixture into the primary circuit, R for perfect gas constant, T_{gas} for the temperature of the gaseous mixture in the primary circuit assumed to be 1800 K, V_{prim} for the volume of the primary circuit and C_d the discharge coefficient of the break imposed at 0.62. Complementarily, the number of moles resulting from the boiling of the core materials results from their heating up to their melting point and then up to their boiling point. Though the dynamic of the overheating up to the melting point of the various core materials have been carefully calculated for slower scenarios also considered in this study, for concision purpose, this first phase of the scenario is not presented here. Therefore, in order to be conservative, the initial core temperature is considered to be equal to the decomposition temperature of the SiC, that is about 2800°C. At this temperature, the fuel is fully molten but remains encased in the cladding because its vapour pressure remains weak as presented on Figure 11. Moreover, considering this initial temperature, the core power is fully dedicated to SiC decomposition at a constant temperature and at a high enthalpy, that is without any possible feedback on reactivity, thus enabling a large power escalation (the Doppler does not act since the temperature is constant and the enthalpy stored in the core materials is very high and available for melting and boiling). Thus, the mass of materials dm_{phase} transformed into another phase during a time step dt by boiling or melting can be linked to the core power by the equation into which the volumic fraction of each material should be respected:

$$dm_{phase} = X_{vol} M \frac{P_{core} dt}{\Delta H_{phase}}$$
 (9)

where T constant like for the boiling or the decomposition of SiC (but with T that can vary from solidus to liquidus temperature for (U,Pu)C for instance) and with ΔH_{phase} (in J/mol) the heat of phase change, P_{core} the core power, X_{vol} the volumic fraction of the material transformed and M its molar mass.

Outside of the phase changes period of the accident, the averaged core temperature evolution dT during a time step dt is linked to the core volumic power by neglecting the thermal transfer during such a fast heating:

$$dT = \frac{dt P_{vol}}{(\rho_{comb} C p_{comb} X_{fuel} + \rho_{SiC} C p_{SiC} X_{SiC})}$$
(10)

where ρ_i , Cp_i and X_i are respectively with respect to the compound i, its density, its heat capacity and its volumic fraction. At each time increment, the temperature obtained in (10) is reported in (6) in order to assess the reactivity that is used in (5) in order to have the core power taken into account in (9) and (10). Table 2 has been used for the numerical applications presented in section 4.2. When the vapour pressure of the core materials exceeds the total pressure in the primary circuit, it is assumed in the model that the core power is consumed for the boiling of the liquified materials (equation (9)) up to the reach of a new thermodynamic equilibrium). The vapour pressure of the liquid composed of the core materials calculated with the Thermocalc code are presented on Figure 11.

(U,Pu)C SiC Volumic fraction 22.4% 26.4% Densisity 12700 kg/m 3200 kg/m 270 J/kg/K 1300 J/kg/K 2420 K 3070 K solidu 2654 K 3070 K Heat of liquefaction 433.7 kJ/mol 74 kJ/mol Heat of vaporization (mixture) 280 kJ/mol

Table 2 Core main thermophysical properties (Thermocalc calculations)

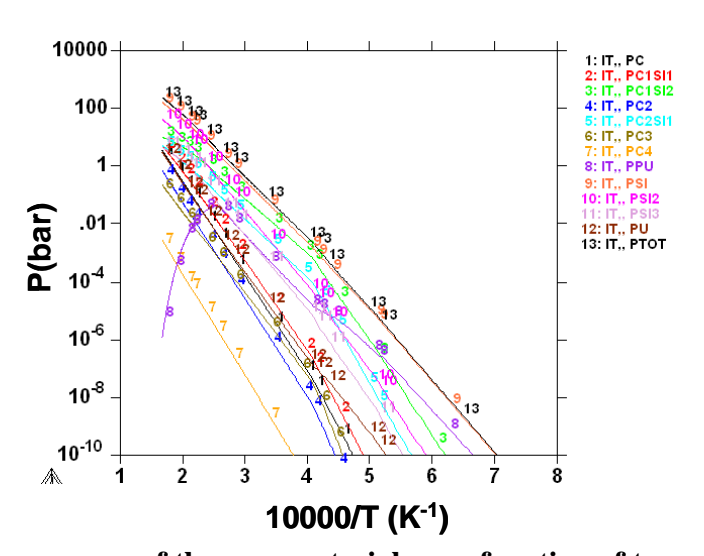


Fig. 11 Vapour pressure of the core materials as a function of temperature

According to Figure 11, the main contributor of the vapour pressure of the core materials consists in the Si vapour resulting from the SiC decomposition and it can be approximated by:

$$P_{\text{sat}}(T) = A \times \exp(-\frac{B}{T}) \qquad (11)$$

with A = $3.37 \cdot 10^{-7}$ and B = 57530 if T<2380 and A = $1.19 \cdot 10^{-6}$ and B = 49570 if T>2380.

4.3 Application to the GFR 2400 (with a time step dt = $50 \mu s$)

As observable on Figure 12, the power excursion calculated thanks to this very simplified model is very large and the thermal energy released and the primary circuit pressure are very sensitive to the reactivity postulated for the accident. As a result, the final pressure rises up to 8 bars only if only 1.9 \$ are inserted whereas it rises up to 26 bars for 2.1 \$. Globally, this modelling is quite conservative since it does not consider the thermal exchanges (all the power is available for material boiling without any effect of thermal losses that are very large by radiative transfers at this temperature) and since it does not consider neither the reactivity decrease due to fuel dispersion. Oscillations observable on the left side of Figure 12 result from the thermodynamic flash of the oversaturated liquid in the core.

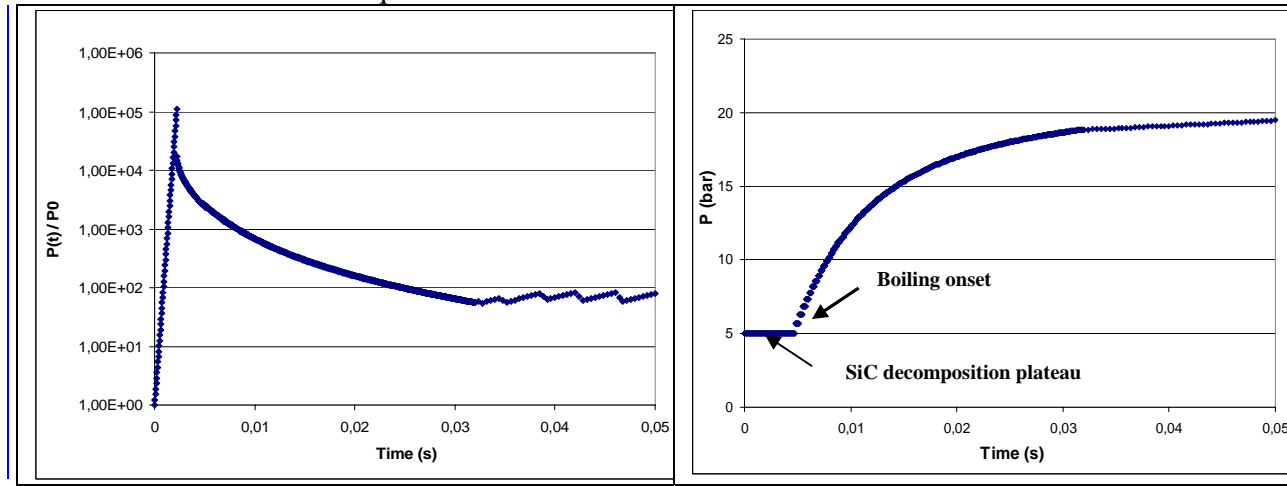


Fig. 12 Core relative power (left side) and primary pressure evolution (right side)

The remarkable feature of the results deals with the pressure peak that not exceeds the nominal pressure of the vessel according to our approximate calculation. The effect of the coupling between the pressure and the temperature loadings of the vessel before the pressure escalation would be interesting to assess in order to conclude on the capability of the vessel to withstand the pressure peak consequently to its prior overheating before the power excursion. The effects of possible dynamic loadings associated to local pressure peaks due to possible local shock wave focusing and reflexion should also be interesting to assess in order consolidate the present results. Finally, an improvement of this preliminary 0-D modelling would be to include in a more spatially refined approach, the thermal exchanges and the reactivity decrease induced by displacement of fuel during the boiling of the core materials.

5. Conclusions

As a complement to previous investigations carried out on beyond design accidents of the GFR 2400, the studies presented in this paper deals with the possibility of prevention of core degradation and with a very rough and preliminary assessment of the vessel pressurization in case of a postulated large and instantaneous reactivity insertion. The accident investigated regarding the aspects aforementioned is the bounding case for a SB-LOCA combined with the reactor shutdown failure. It is worth noticing that the main interest of the work relies on the of the coupling between the various physical phenomena treatment (thermalhydraulics/neutronics/physico-chemistry) with a simplified approach associated to assumptions justified in the way of providing preliminary order of magnitude in the conservative direction. First, thanks to an optimized control of the core cooling with an adapted operating of cooling systems, the accident investigated could be controlled during approximately 1 h 30 mn without any irreversible loss of the core geometry due to material liquefaction. The decrease of the liner thickness has been calculated thanks to thermochemical models validated on experimental tests and this calculation indicates that even in the region of the core without liquefaction, the whole thickness of the liner would be consumed in approximately two hours, thus leading to a loss of cladding tightness. Moreover, if a large reactivity of about 2 \$ was suddenly inserted in the core caused by an hypothetic event occurring after the unprotected SB-LOCA investigated without the counter-measures envisaged in this paper, a pressurization of the vessel would occur but the pressure would remain lower than the nominal pressure of the primary circuit without regards to the possible dynamic loadings. This last preliminary assessment is aimed at filling the lack of a dedicated severe accident code for the GFR but should be further refined.

6. Acknowledgment

The authors would like to thank the Nuclear Support and Innovation Division of the CEA, AREVA and EDF which support this project as well as the RAGAZ project manager and all the engineers that contribute to the GFR design and safety. Finally, all the members of the GFR severe accidents working group (G2AG) of CEA also deserve our acknowledgments for their implication and the quality of their work.

7. References

- [1] J.Y Malo & al., "Gas Cooled Fast Reactor 2400 MWth, status on the conceptual design studies and preliminary safety analysis", proceeding of ICAPP 2009, Tokyo, Japan, May 10-14, 2009.
- [2] F. Bertrand & al., "Preliminary Safety Analysis of the 2400 MW Gas-Cooled Fast Reactor", proceeding of ICAPP 2008, Anaheim, USA, June 8-12, 2008.
- [3] F. Bertrand & al., "Preliminary transient analysis and approach of hypothetical scenarios for prevention and understanding of severe accidents of the 2400 MWth Gas-cooled Fast Reactor", N13P1057, Proceedings of NURETH-13, Kanazawa City, Japan, September 27-October 2, 2009.

- [4] C. Bassi & al. "Level 1 probabilistic safety assessment to support the design of the CEA 2400 MWth gas-cooled fast reactor", Nuclear Engineering and Design, Iss. 240, 2010, pp.3758-3780.
- [5] M. Robert & al., "CATHARE2 V2.5: A fully validated CATHARE version for various applications", proceedings of NURETH-10, South Korea, 2003.
- [6] O. Widlund & al., "Overview of Gas Cooled Reactor applications with CATHARE", proceedings of NURETH-11, Avignon, France, October 2-6, 2005.
- [7] F. Bentivoglio & al., "CATHARE simulation of transients for the 2400 MW Gas Fast Reactor concept", proceedings of ICAPP 2009, Tokyo, Japan, May 10-14, 2009.
- [8] J.M. Ruggieri & al., "ERANOS 2.1: International Code System for GEN IV Fast Reactor", proceedings of ICAPP 2006, Reno, USA, June 4-8, 2006.
- [9] http://www.thermocalc.com
- [10] A. Berche & al. "Thermodynamic study of the U-Si system", Journal of Nuclear Materials, Vol 389, Iss 1, 15 May 2009, pp.101-107.
- [11] V.S. Eremeev & al., Proceedings of the Symposium on Thermodynamics with Emphasis on Nuclear Materials, V.II, IAEA, Vienna, 1966, p. 161.
- [12] J. Roger & al., "Thermal reaction of SiC films with tungsten and tungsten-rhenium alloys", Journal of Material Science, Vol 43, 2008, pp.3938-3945.
- [13] H. Yamano & al., "A three-dimensional neutronics-thermohydraulics simulation of core disruptive accident in sodium-cooled fast reactor", Nuclear Engineering and Design, Iss 239, 2009, pp.1673-1681.
- [14] J. Bussac and P. Reuss, "Traité de neutronique", collection enseignement des sciences, 1985, Editions Hermann.
- [15] C.J.H. Van Den Bosch & al., 1997. TNO Yellow Book, Method for the calculation of physical effects CPR 14E", Sdu Uitgevers.